Distributed and Transient Electro-thermal Modeling and Its Impact on RF Predistortion

Patrick Roblin*
Wenhua Dai
The Ohio State University

THE OHIO STATE UNIVERSITY

Outline

- Introduction
- Electrical modeling
- Part I: Image method thermal modeling and distributed thermal model
- Part II: Transient thermal response and memory effects in RF predistorter
- Part III: Experimental results on memory effects

Introduction

•High power devices suffer from self-heat during operation, which affects its electrical performances.

•Most of the power device models use simple low pass RC circuit to model the self-heating The non-uniformly distributed temperature across the power device requires a model to capture the temperature distribution.

•Dynamic self-heating due to the low frequency modulation envelop causes thermal memory effects.

•Memory effects are categorized into thermal and electrical memory effects. Via simulation we can identify their separate contributions.

•Temperature rise in a multilayer material involves fast and slow time constants. A multiple RC time-constant model is required to capture the complete device electro-thermal dynamic.

Thermal Rth Measurement

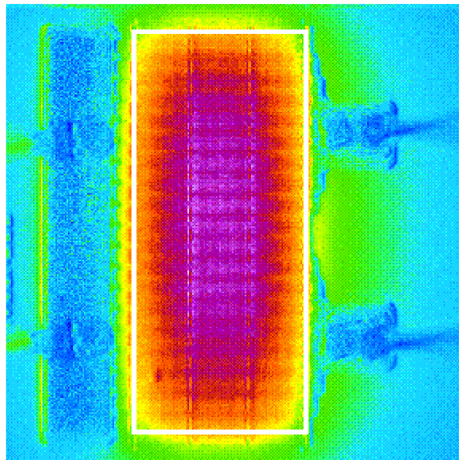

20 fingers
6.34C/W

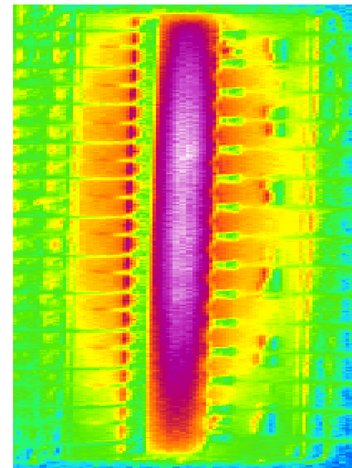

144 fingers
1.44 C/W

Rth is obtained through steady state temperature measurement
- calculated using an average device temperature
- exhibits a nonlinear scaling with the device size

Thermal Time Constant Measurement

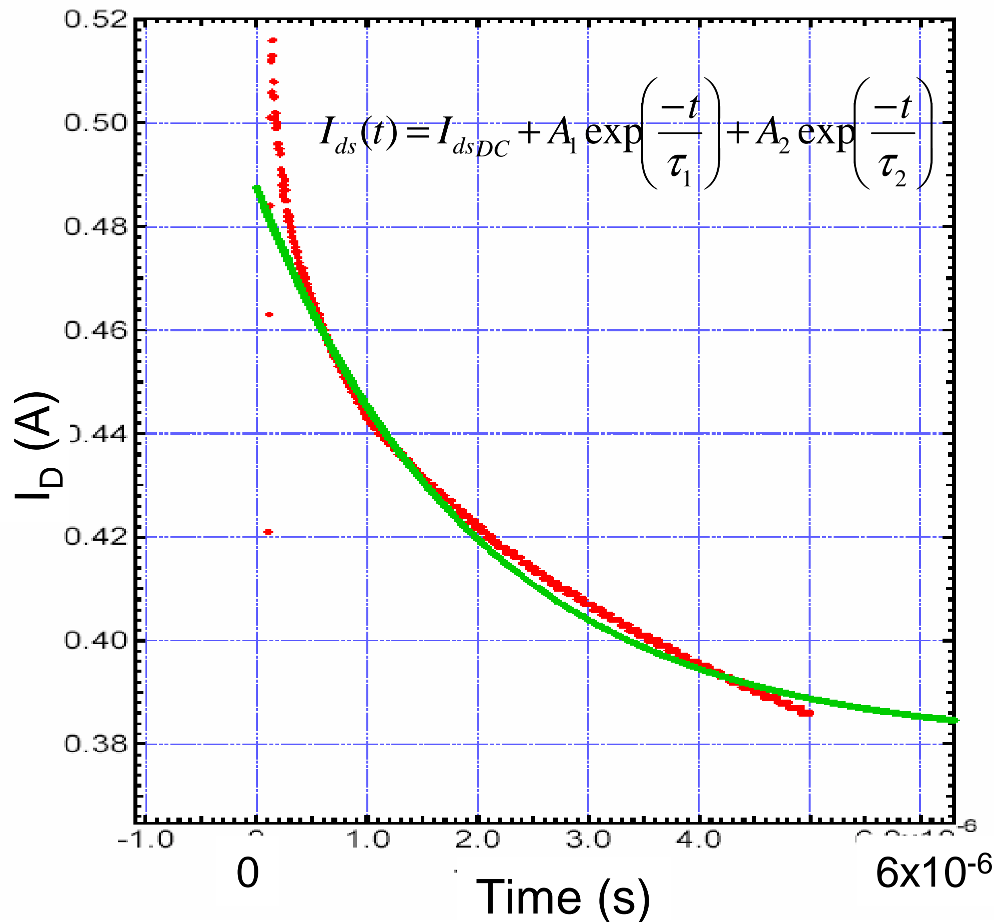

Thermal time constant can be obtained through pulse IV measurement: the Drain current decrease/increase due to the heating

- Measured rise time maybe affected by C_{gs}, L_s, and the power supply.

- Two competing temperature dependences (Vth, mobility) may cancel each other, resulting in a reduced thermal dependence.

Large Signal Electro-Thermal Model

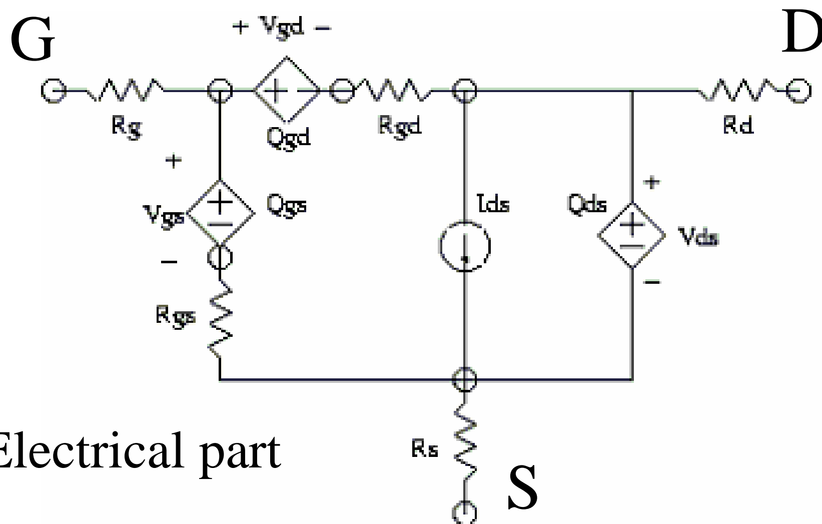

Electrical part

Thermal part

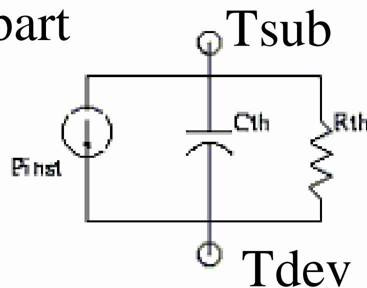

- Nonlinear large signal electrical model
- IV characterization from both iso-thermal and pulse measurement
- S-parameter characterization from iso-thermal measurement
- Parasitics from cold FET measurement
- Simple RC circuit to model the temperature response

Electro-Thermal IV for LDMOSFET

Vgs from 4 to 6.5 in steps of 0.25 V

Temperature in C

Drain Current in Amps

Extrinsic Vds in Volts

Model Verification Using Scattering Parameters

OSUFET B-spline model (2 bias points)

AET analytic model

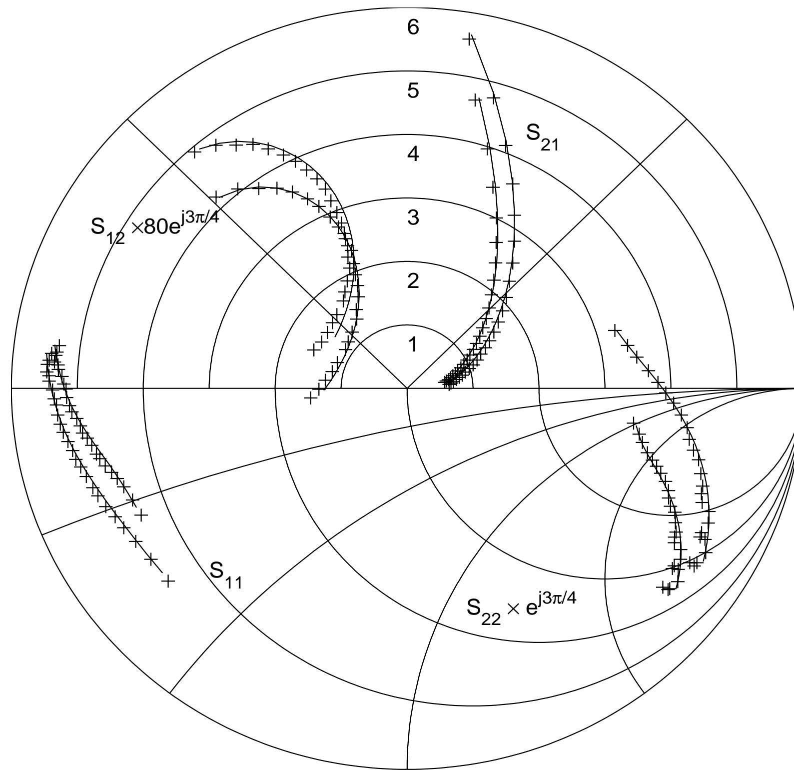

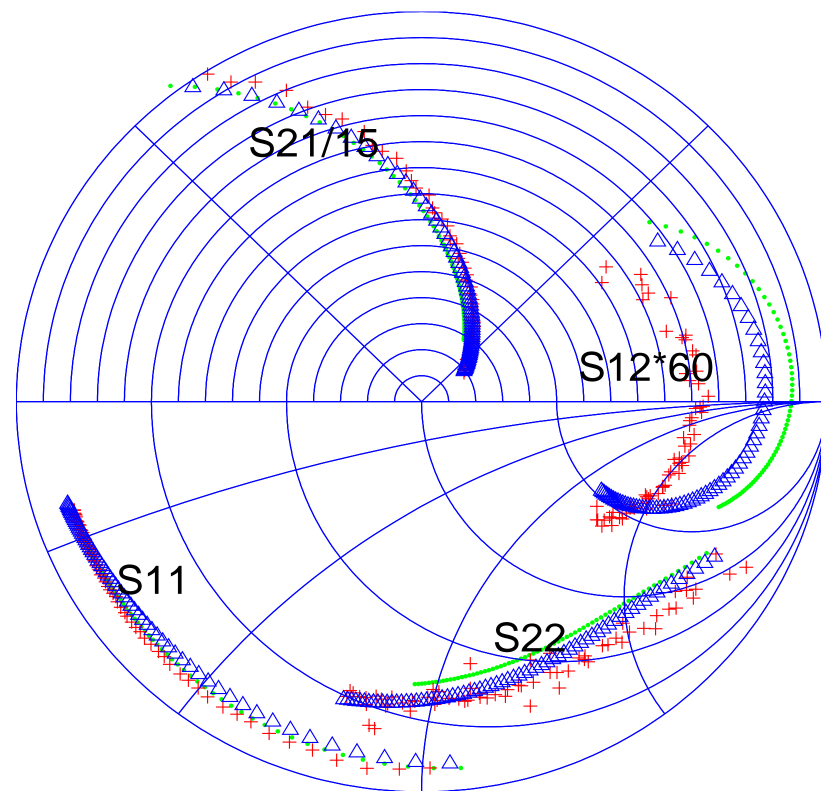

THE OHIO STATE UNIVERSITY

Model Verification Through Loapull

Loadpull test bench

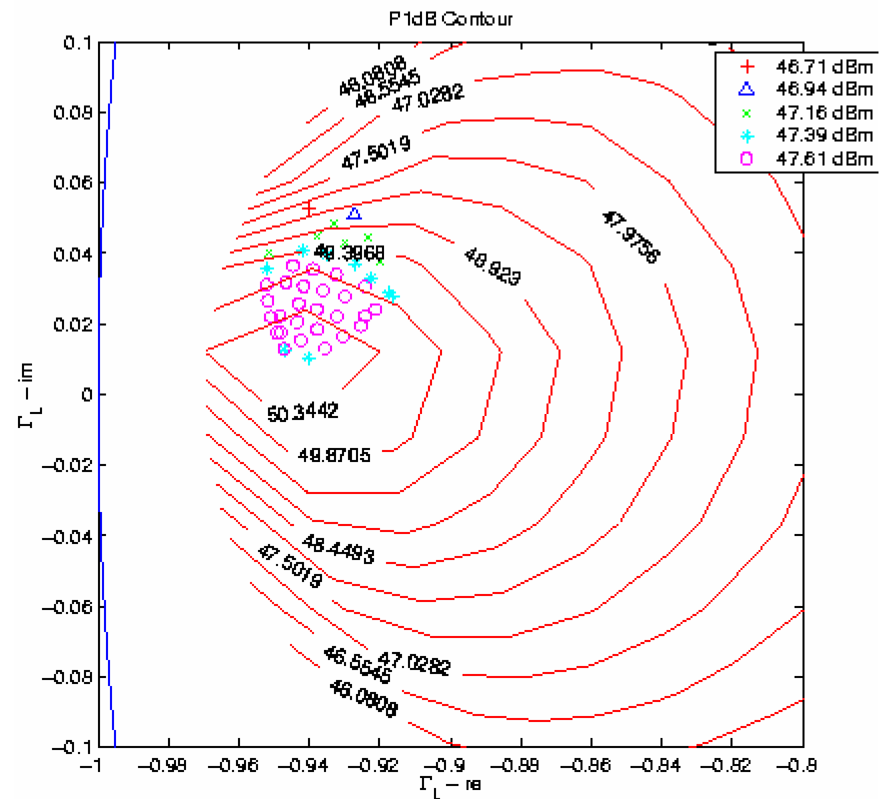

Model Verification using the Harmonic Response of an Amplifier

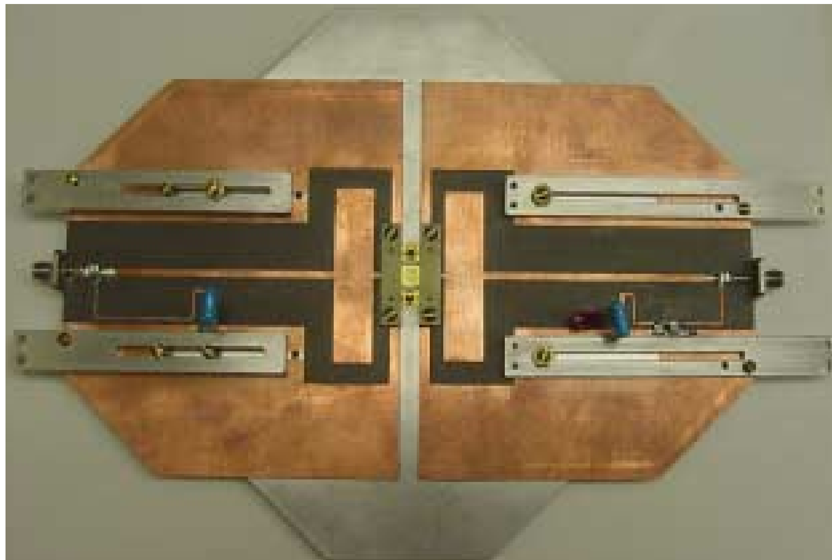

1 W amplifier

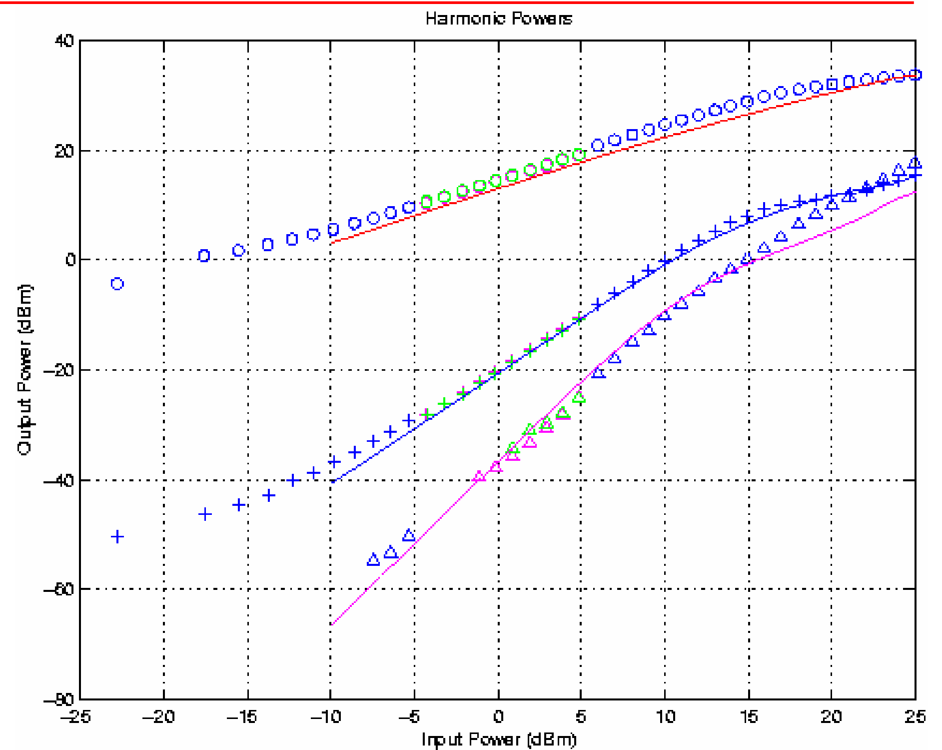

THE OHIO STATE UNIVERSITY

Part I: Lateral Thermal Model

- 3D steady state temperature calculation
- Experimental Results
- ADS implementation
- Results

Image Method for Steady State Temperature Field

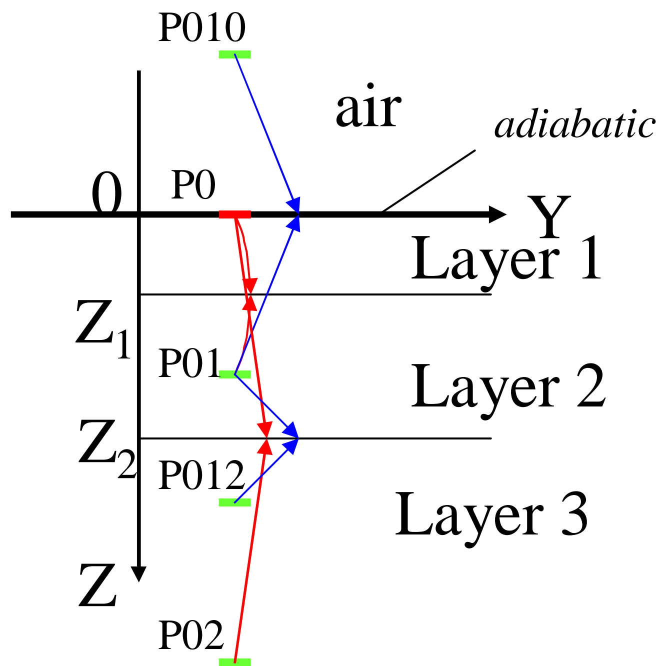

Green function: $dT(\mathbf{r},\mathbf{r}') = \frac{q_s}{4\pi k \Delta \mathbf{r}} dx' dy'$

B.C. : $T(Z = Z_1^-) = T(Z = Z_1^+)$

Image sources are formed so that B.C be satisfied

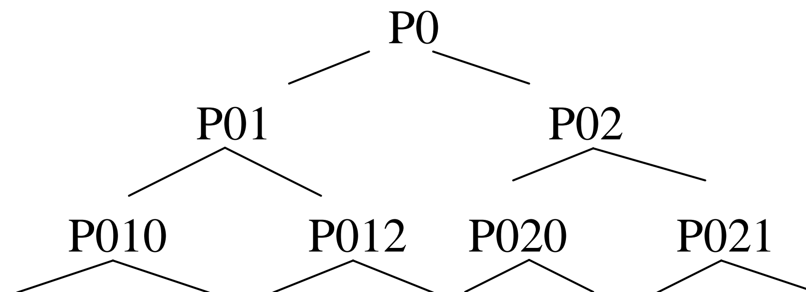

Based on: Rinaldi, N, "Generalized image method with application to the thermal modeling of power devices and circuits" *IEEE Trans. on Electron Devices, Vol. 49, No. 4, p. 679, 2002.*

Non-Linear Scaling of Average Rth

Gate Width	# of cells	Rth ^{o}C/W
3 μm	1	6.17
12 μm	4	2.79
48 μm	16	1.07

2.8 ^{o}C/W measured in our testbed for 12 μm devices.

The device models cannot rely on linear scaling rule for Rth because of the lateral heat flow.

Distributed Thermal Model

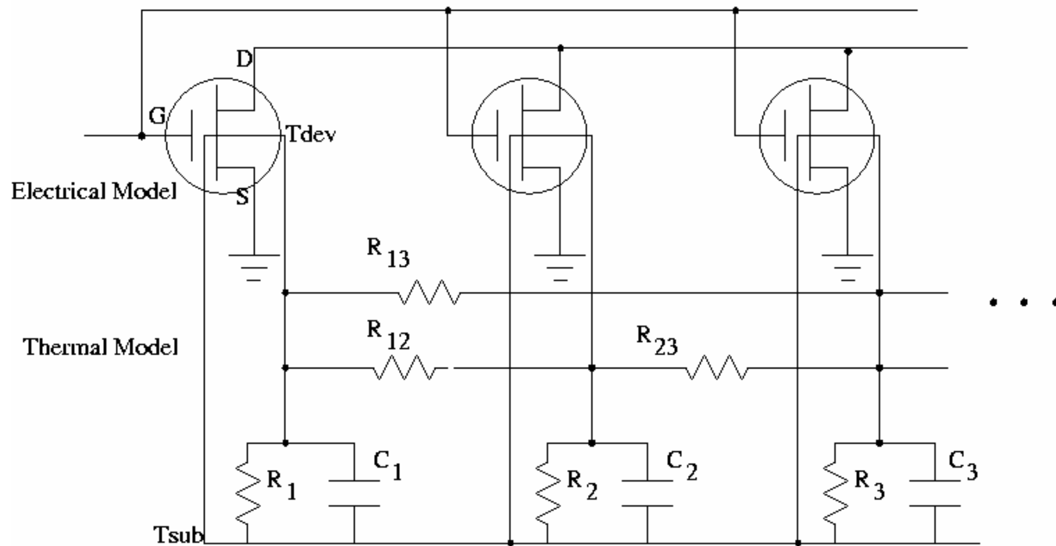

Mutual heat flow is modeled by mutual thermal resistance

Extraction from Rth matrix calculation through image method

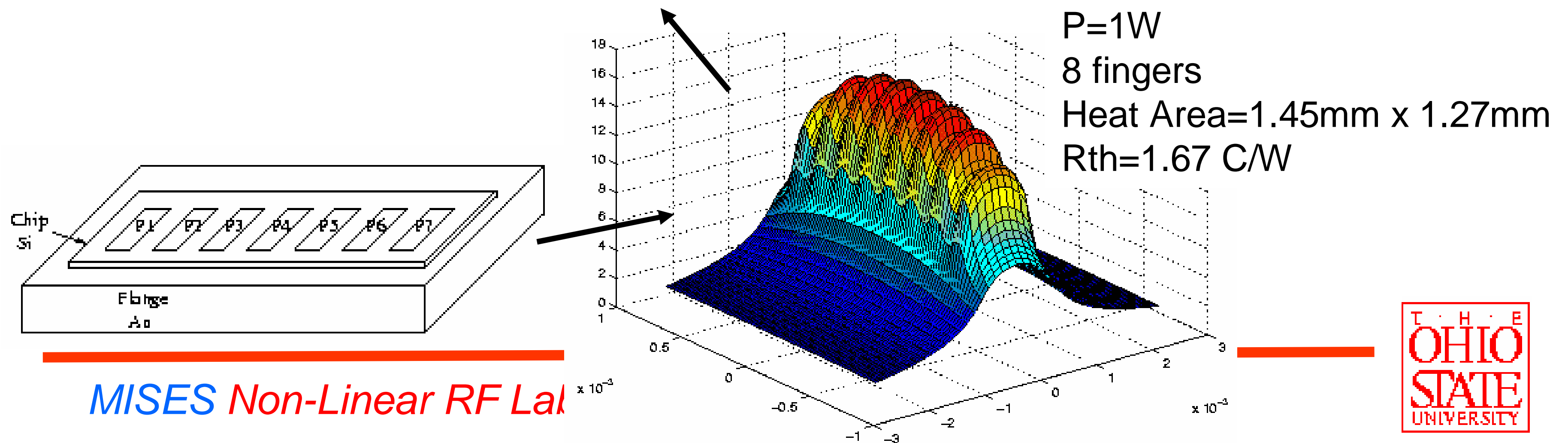

Distributed Electro-Thermal Model Reduction

- Fingers are symmetrical to the center
- Number of fingers is reduced by half
- Each finger has its size doubled
- Rth matrix folded, each Cth is doubled

$$\begin{bmatrix} \frac{R_{1,1}+R_{1,n}}{2} & \cdots & \frac{R_{1,n/2}+R_{1,n/2+1}}{2} \\ \vdots & \ddots & \vdots \\ \frac{R_{n/2,1}+R_{n/2,n}}{2} & \cdots & \frac{R_{n/2,n/2}+R_{n/2,n/2+1}}{2} \end{bmatrix}$$

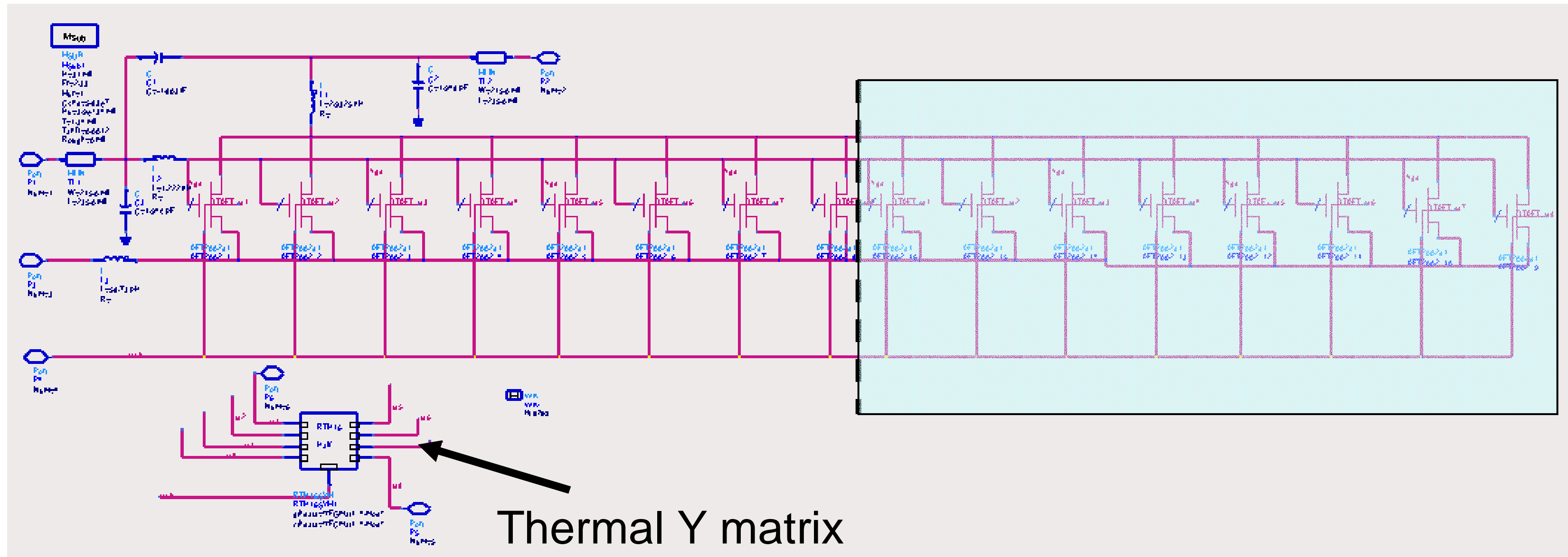

Thermal Y matrix implemented in ADS

Transient Simulation with Distributed Model

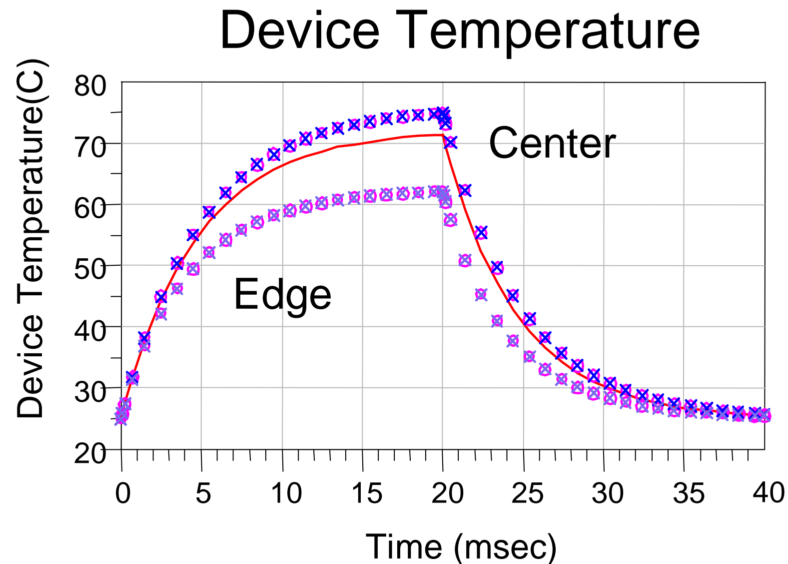

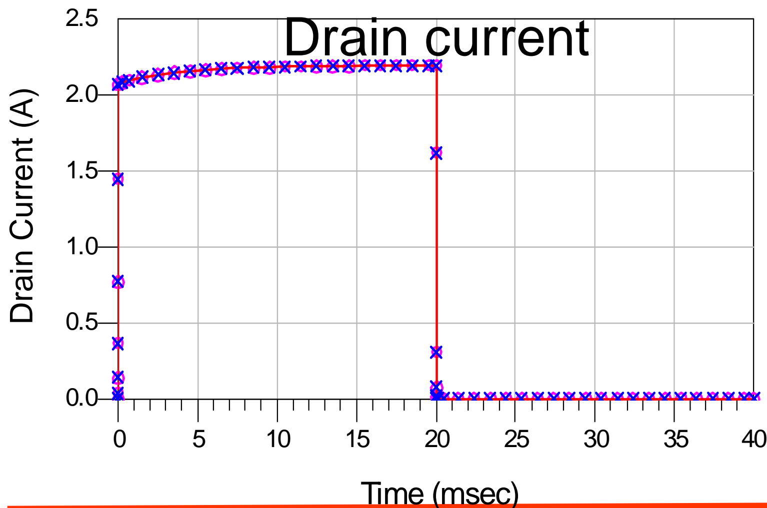

3 models: non-distributed,
distributed,
distributed half

Red (line) – one-finger approximation
Magenta (o) – distributed 16 fingers
Blue (x)– distributed 8 fingers

- Temperature distribution is seen in distributed model
- Non-distributed model reports the averages temperature across the fingers
- Overall electrical behavior is consistent, indicating the non-distributed model has enough accuracy

Results for Part I: Lateral Distributed Thermal model

- A recently reported image method can facilitate the thermal modeling of multilayer devices to account for lateral distributed thermal effects in large multifinger devices.
- Model was implemented in a circuit simulator using a distributed lateral thermal model using a single RC time constant for each finger.
- Temperature distribution can be reproduced. This is useful in applications where accurate temperature information is required.
- However the overall electrical behavior can be modeled with enough accuracy by a non-distributed model reproducing the average temperature.
- An important application of distributed model is however to predict the non-linear scaling of Rth with device area.

Part II: Transient Thermal Modeling and Memory effects

- Approximate transient response with image method
- Multistage RC model for ADS implementation
- Impact of transient thermal model on a RF amplifier with a predistorter
- Results for multisine excitation on 1W and 60W PAs
- Results for IS95 CDMA excitation

Image Method for Approximated Transient Temperature Rise in Multilayer Structure

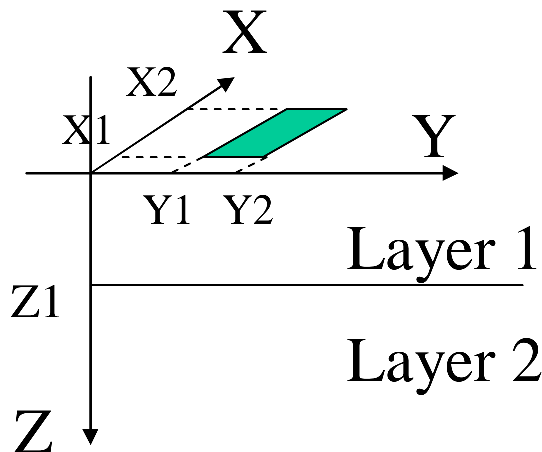

Time dependent Green function of a rectangular heat source:

$$T(x,y,z,t)=\frac{q_s}{4k\sqrt{\pi}}\int_0^{2L}e^{-\frac{z^2}{u^2}}\left[f\left(\frac{X_2-x}{u}\right)-f\left(\frac{X_1-x}{u}\right)\right]\left[f\left(\frac{Y_2-y}{u}\right)-f\left(\frac{Y_1-y}{u}\right)\right]du$$

$$f(x)=\mathrm{erf}(x)$$

$$L=\sqrt{Dt}$$

Boundary conditions:

$$T\left(Z=Z_1^-\right)=T\left(Z=Z_1^+\right)$$ For all t

Approximation 1: when D1=D2, boundary condition is independent of *time*, so that image method can be used

Approximation 2: thermal conductivity of layer 2 is large enough

Transient Temperature Rise

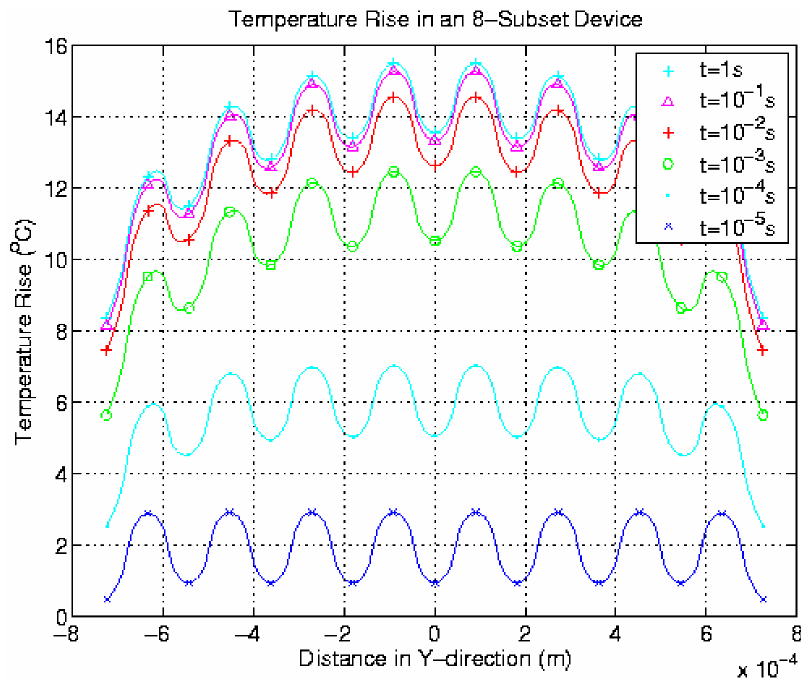

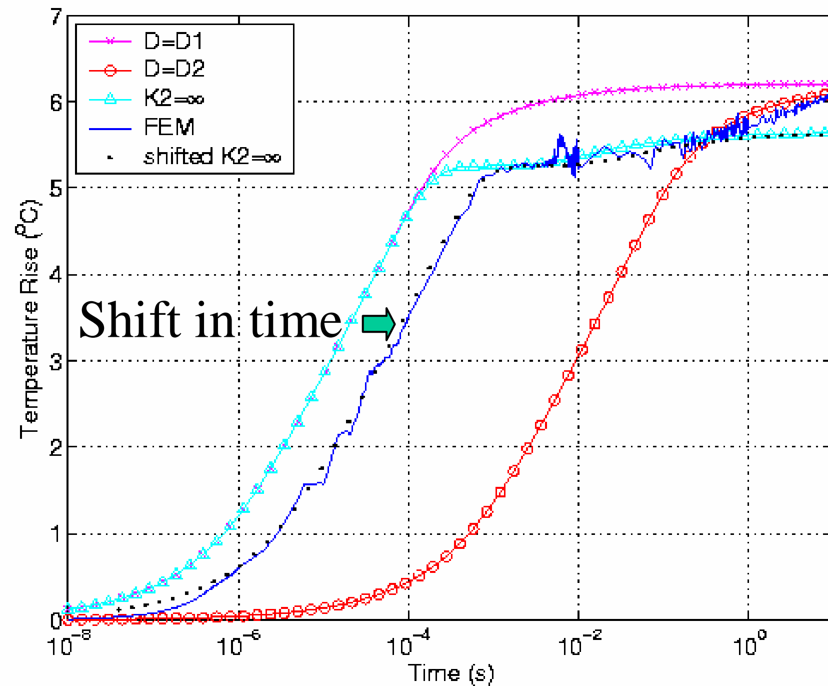

FEM provides 'true' temperature response, long computation time
Image method provides approximated solution

Multi-time-constant Thermal Model

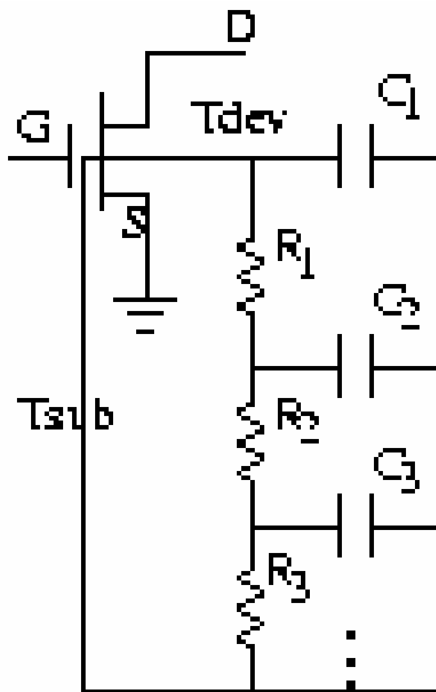

Slow and fast transient temperature rise can be modeled

Rth includes junction, Si chip, flange, and copper block

Extraction from transient temperature measurement/calculation

Thermal Parameter Extraction

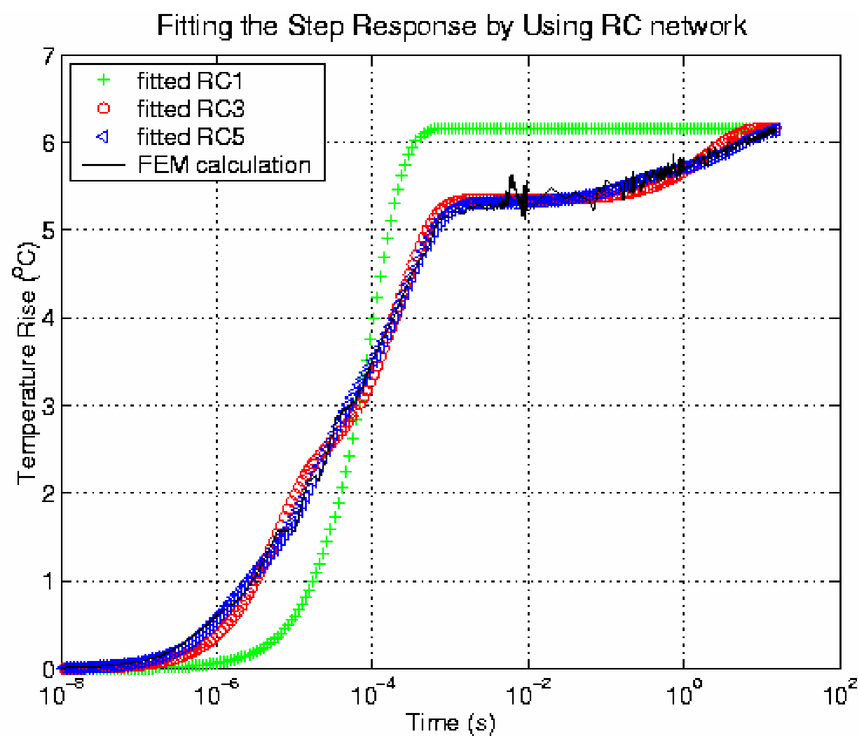

	Rth (Ohm)	Cth (F)
1-stage	6.17	1.60e-5
3-stage	2.36	2.45e-6
	2.98	7.38e-5
	0.83	2.39
5-stage	1.16	1.29e-6
	1.97	9.38e-6
	2.18	1.24e-4
	0.35	5.39e-1
	0.51	8.89

Extracts Rth and Cth by curve fitting in log scale
Constraint total Rth constant

Amplifier

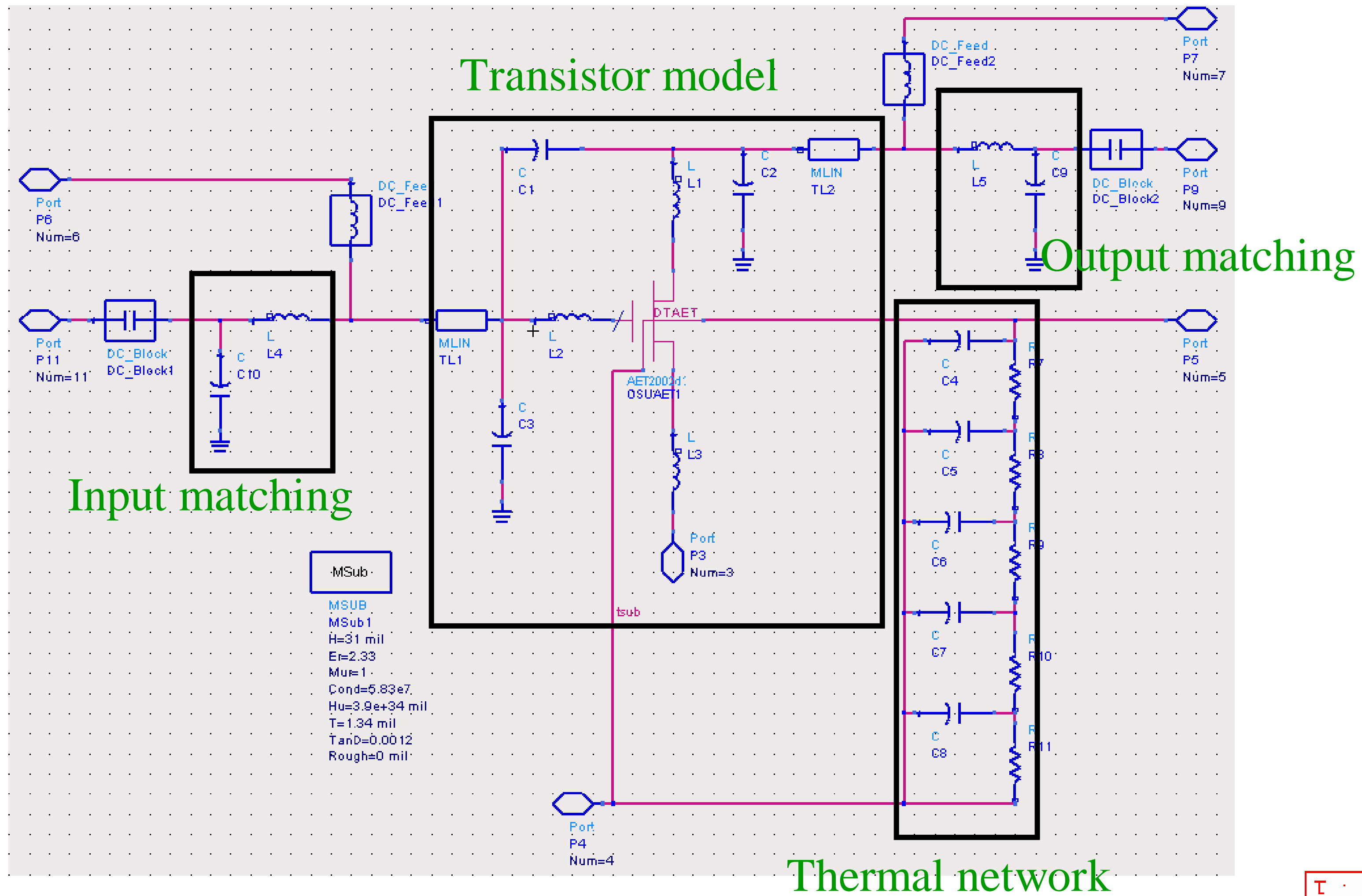

Two-tone Simulation

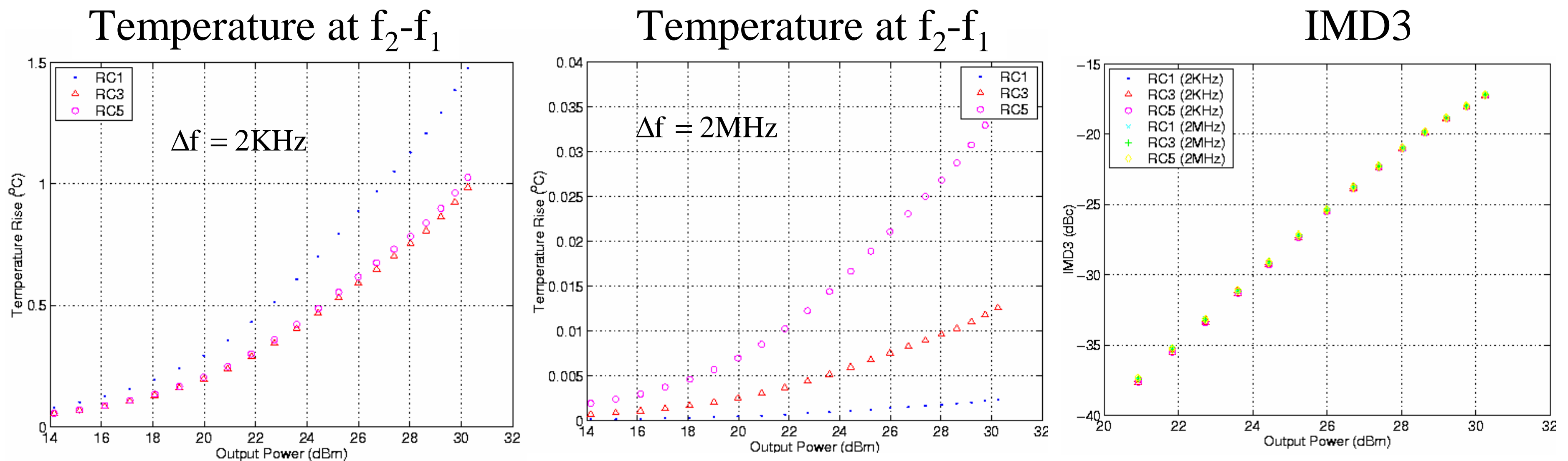

- Low modulation frequency generates bigger temperature variation
- Temperature variations are too small to affect the electrical behavior (IMD3)
- Class A amplifier less sensitive

Thermal Step Response for Devices of Various Sizes

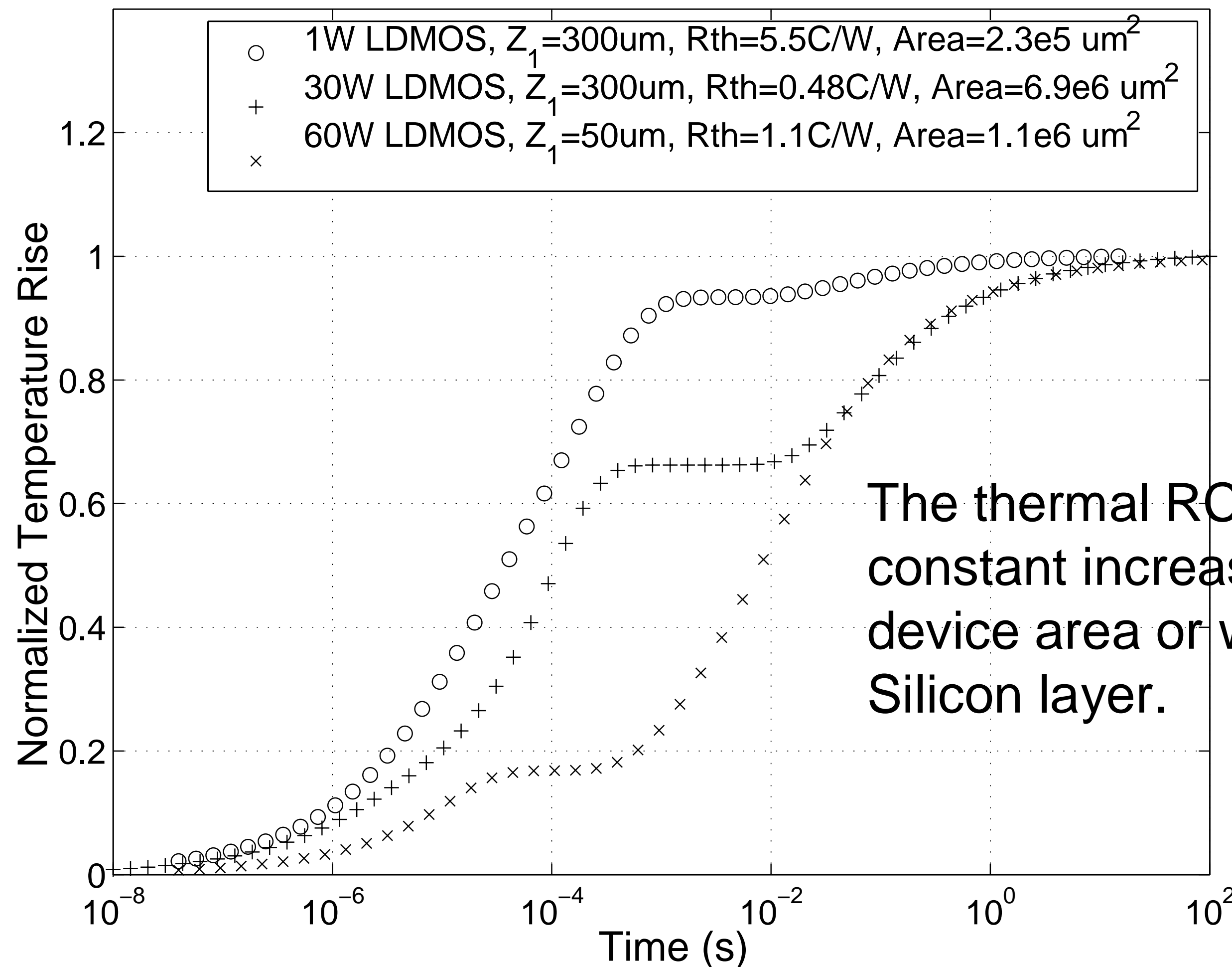

The thermal RC time constant increases with the device area or with thinner Silicon layer.

THE OHIO STATE UNIVERSITY

Impact of Thermal Memory Effects on RF-Predistortion

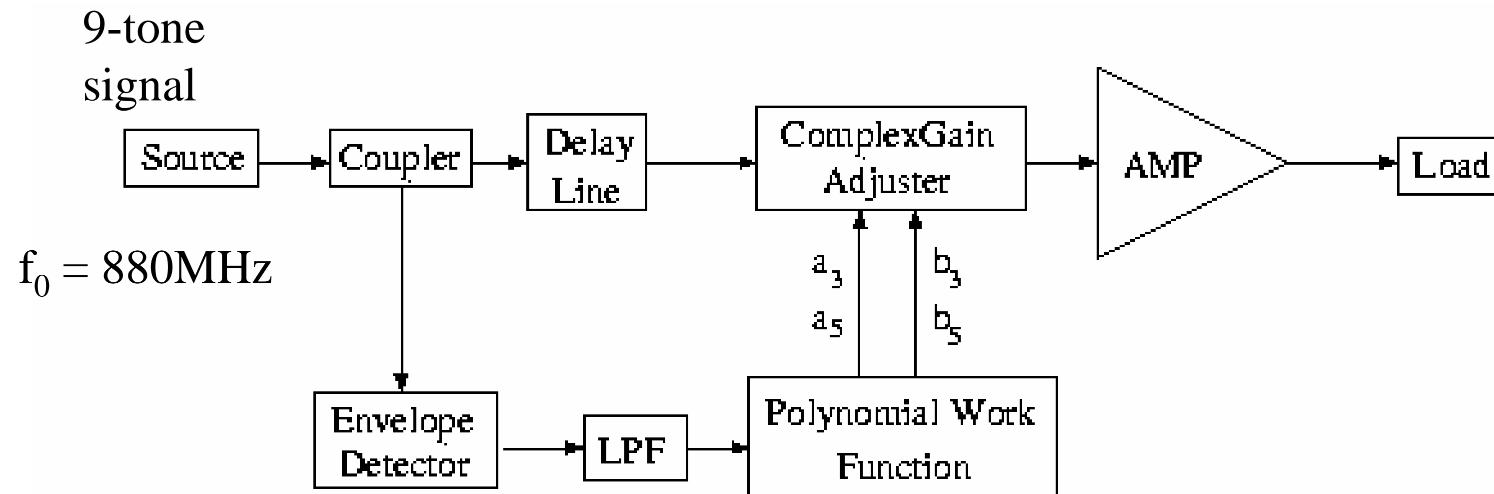

RF predistorter is expected to be more sensitive to low frequency temperature variation

Background and Motivation

From recent studies :

- Memory effects (frequency dependence of non-linearities) in RF PAs (power amplier) degrade the performance of a PA linearization [1]

- The linearization degradation for signals with bandwidth above 1MHz is linked to fast electrical memory effects rather than slow thermal memory effects [2]

[1] J. S. Kenney, W. Woo, L. Ding, R. Raich, H. Ku, and G.T. Zhou,``The Impact of Memory Effects on Predistortion Linearization of RF Power Amplifiers," Proc. of the 8th Int. Symp. on Microwave and Optical Techn.

[2] W. Dai and P. Roblin,``Distributed and Multi-Time-Constant Electro-Thermal Modeling and its impact on ACPR in RF predistortion" ARFTG 62 Conference, Denver, Co., pp. 89-98, Dec. 2003.

FPGA Digital Testbed for RF Predistortion

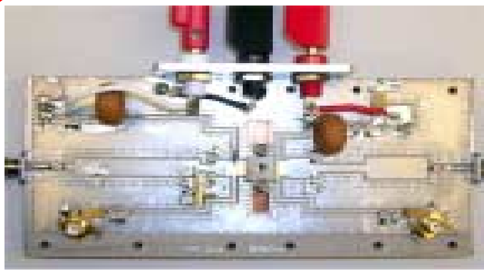

DUT : Power Amplifier

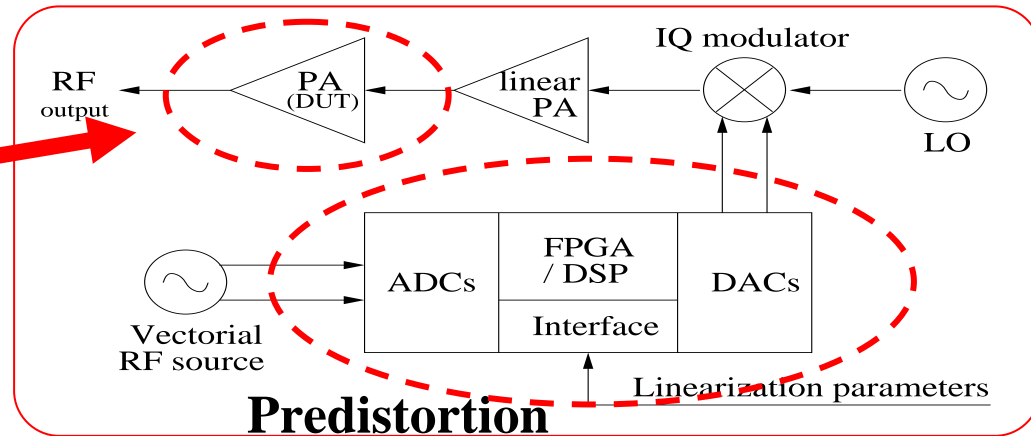

Predistortion

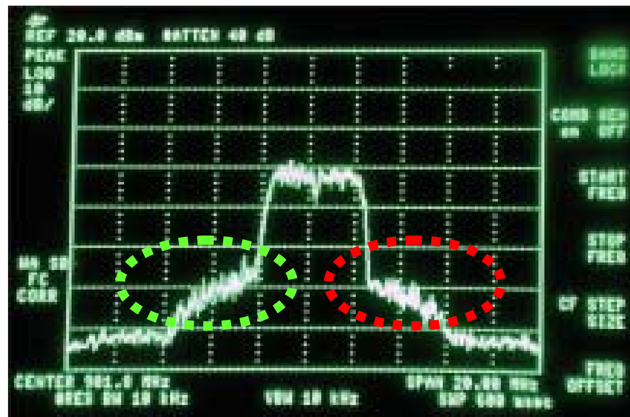

Before linearization

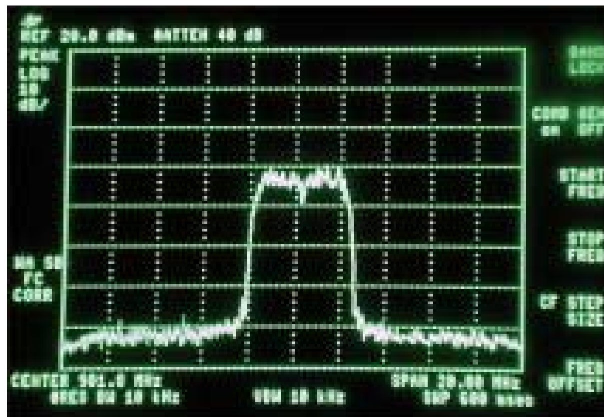

After linearization

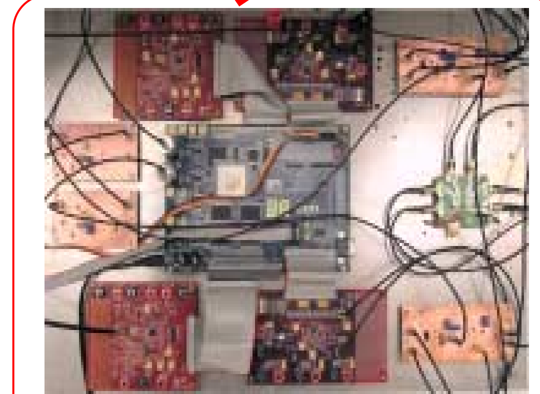

Digital Testbed

RF-Predistorter in ADS

9-tone source signal
Newman's Phase (1965)
f_0=880MHz
PAR=2.6

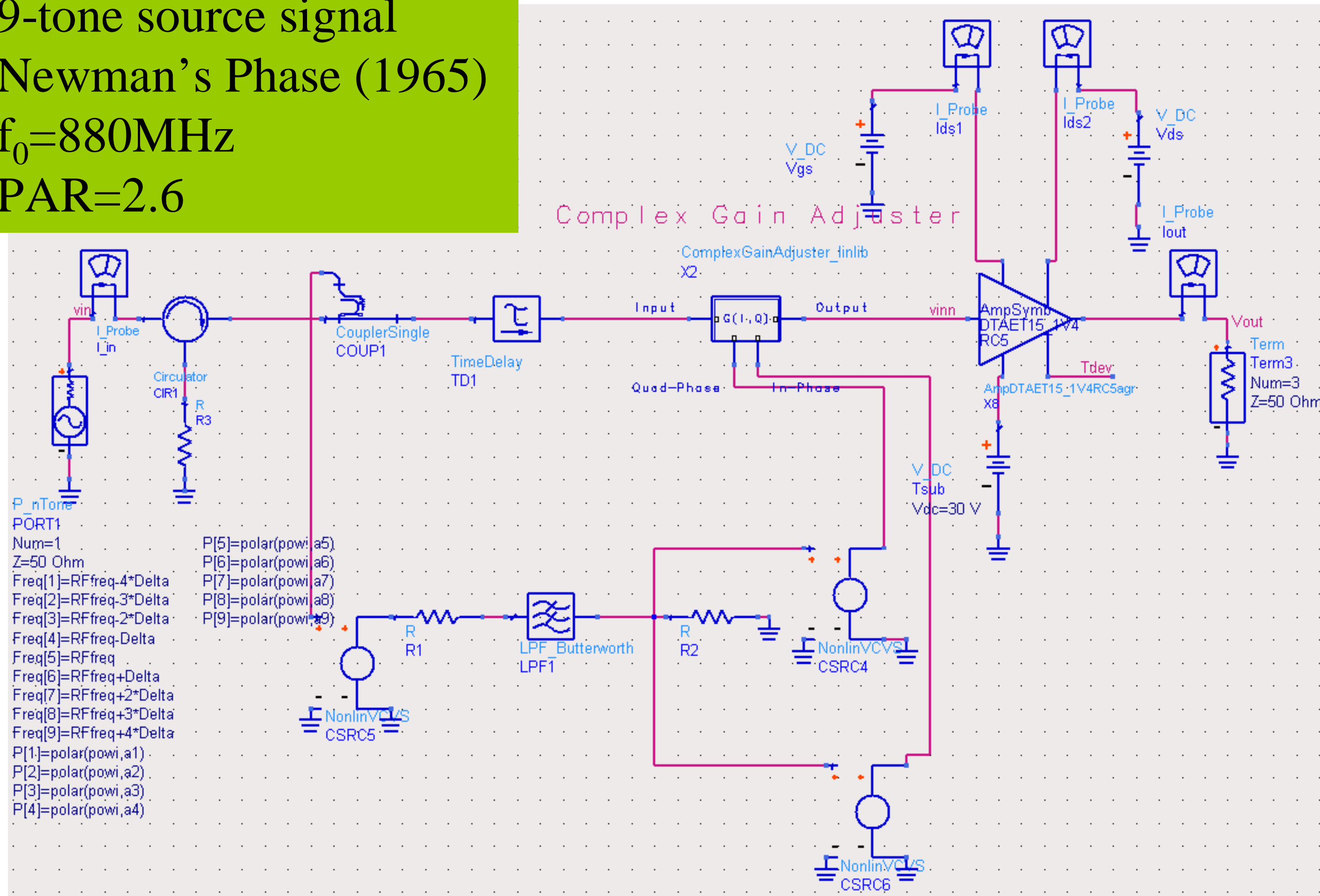

ACPR versus Multisine Bandwidth

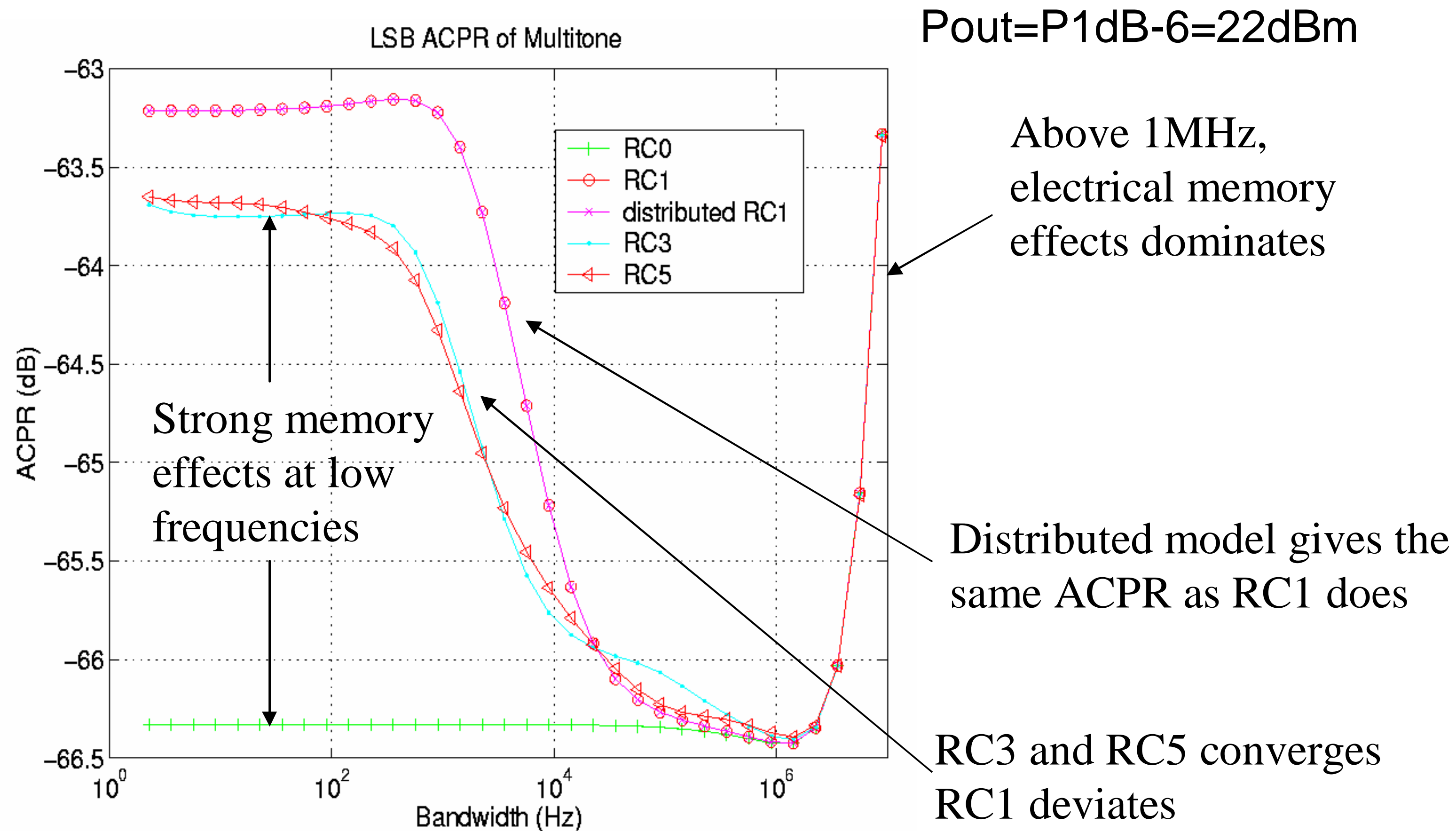

Pout=P1dB-6=22dBm

Above 1MHz, electrical memory effects dominates

Distributed model gives the same ACPR as RC1 does

RC3 and RC5 converges
RC1 deviates

Spectral Regrowth for a 1MHz Bandwidth Multisine

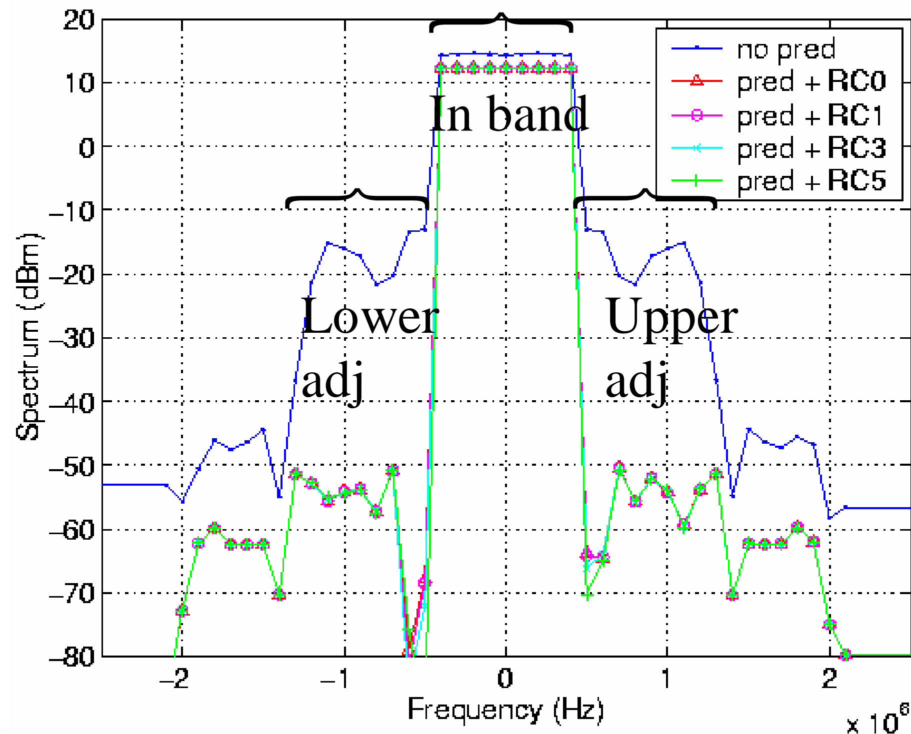

Center freq: 880MHz
9 tones
Tone-spacing: 0.1MHz

	Pout	Lacpr	Uacpr
no pred	24.08	-31.14	-31.12
with pred	21.88	-66.59	-66.47

Small differences between thermal models

$$ACPR = \frac{\text{total power of inband 9 tones}}{\text{total power of adjband 9 tones}}$$

Spectral Regrowth for a 1KHz Bandwidth Multisine

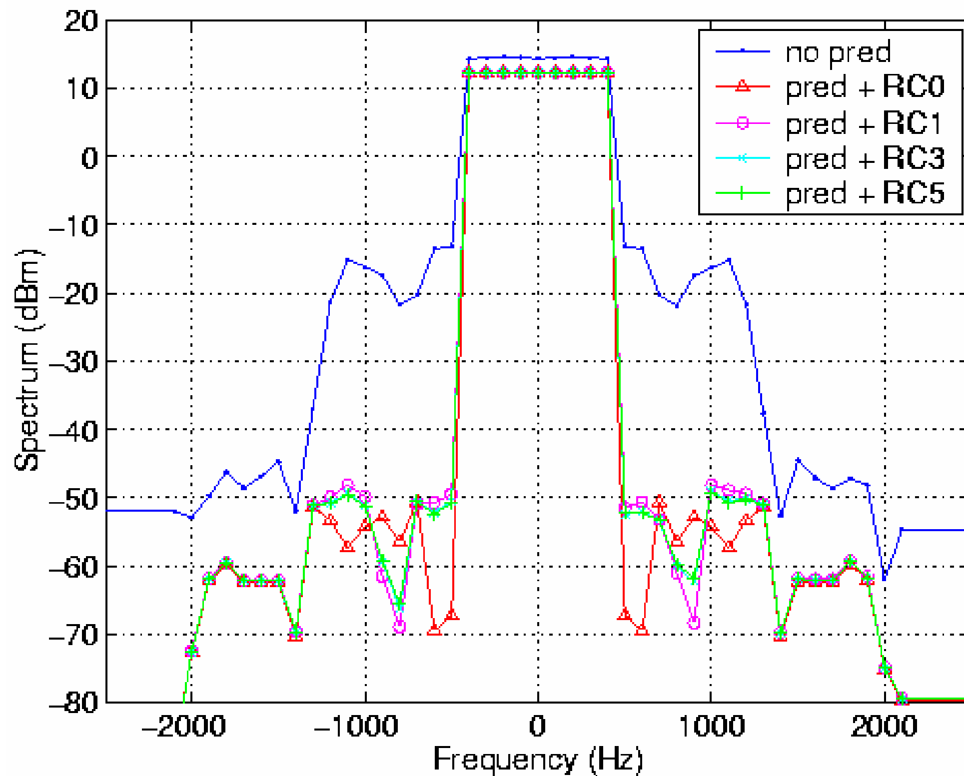

Center freq: 880MHz
9 tones
Tone-spacing: 0.1KHz

	Pout	Lacpr	Uacpr
no pred	24.08	-31.25	-31.32
RC1 pred	21.88	-63.27	-63.46
RC5 pred	21.88	-64.17	-66.39

Noticeable differences up to 3dB between thermal models

$$ACPR = \frac{\text{total power of inband 9 tones}}{\text{total power of adjband 9 tones}}$$

IS95 CDMA simulation

Power level: P1dB-4dB=24dBm

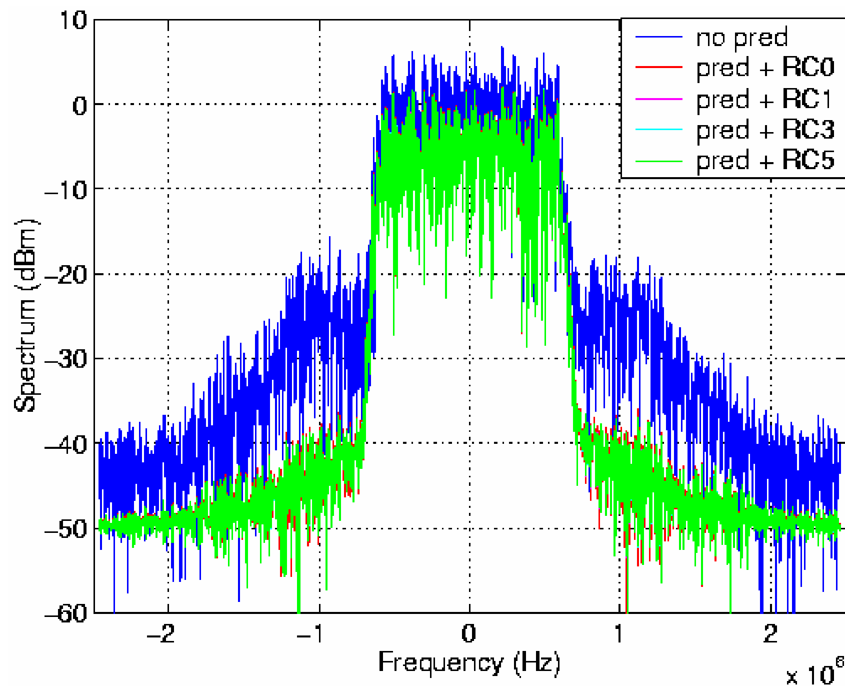

	Direct	RC0	RC1	RC3	RC5
LACPR (dBc)	-44.2	-61.3	-61.6	-61.6	-61.6
HACPR (dBc)	-40.2	-58.9	-59.4	-59.4	-59.4
Pout (dBm)	28.1	24.1	24.0	24.0	24.0

** ACPR defined as power ratio of 30KHz adjband to 1.2288MHz inband

Env simulation of IS95 CDMA signal
Bandwidth: 1.2288MHz
Time: 0 – 0.833ms
Freq resolution: 2.4KHz
Frequency span: 5MHz
Input PAR: 7.39

Improved thermal model has a negligible effect for a class A with IS95

Conditions for Strong Thermal Memory Effects

- ACPR needs to be strongly sensitive to fluctuations of the temperature

Note: ACPR is more sensitive to Delta T when using a predistorter (by a factor 10)

Note: sensitivity is 0.43dB/C (small)

- Amplifier needs to exhibit a large fluctuation (variance) of the temperature

Note: temperature fluctuation increases with input RF power and Rth

Temperature Variation

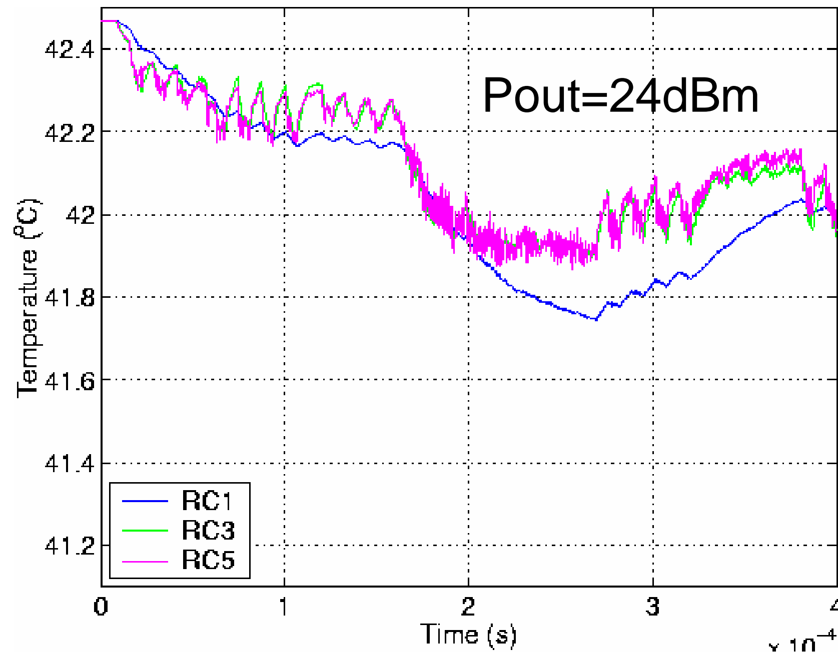

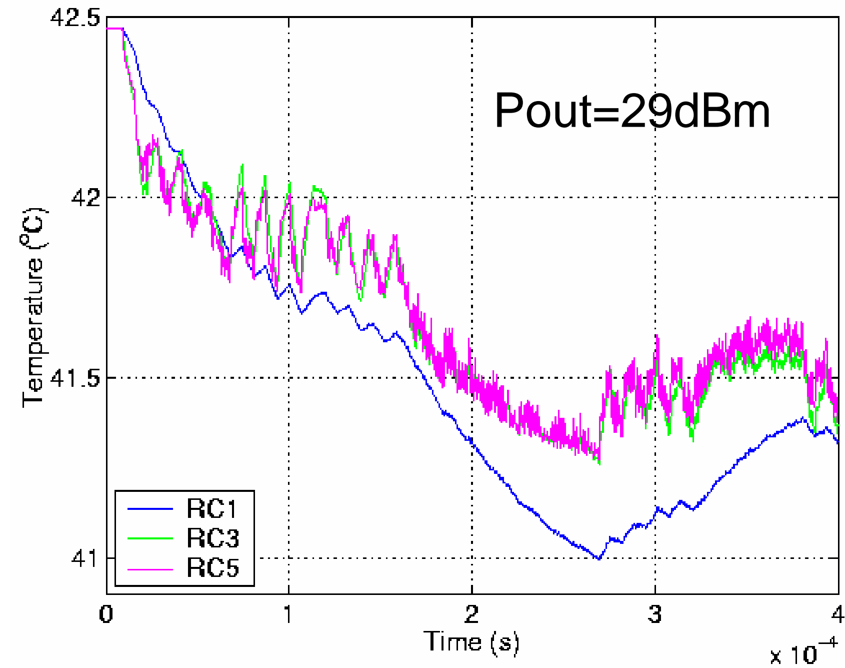

RC5 and RC3 have converged,
But RC1 is not accurate.

	low frequency ΔT	high frequency ΔT
RC1	1.5 C	0.01 C
RC5	1.25 C	0.25 C

Temperature variations are small for CDMA source in the class A amp considered here.

Sensitivity of ACPR to Temperature with Predistorter

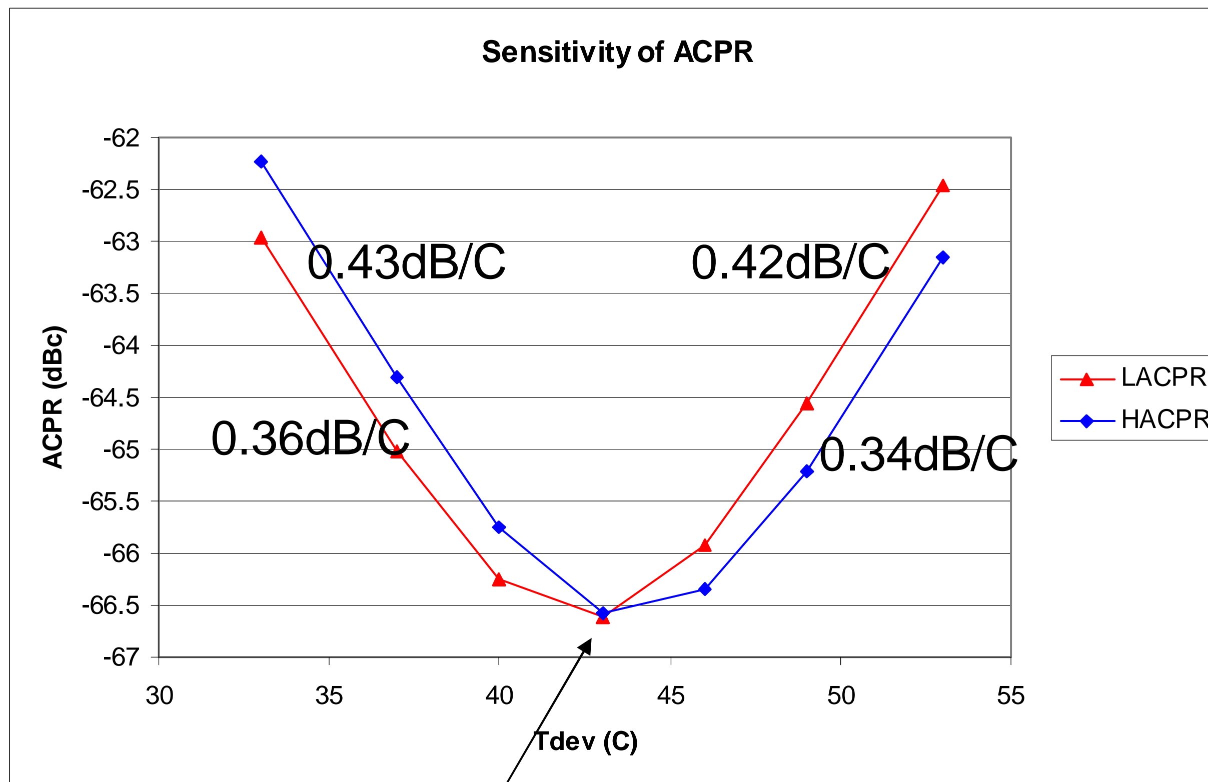

Measure ACPR vs. Tsub in RC0 model

Sensitivity is non-negligible

Predistorter optimized at this temperature

Class AB 60W Amplifier

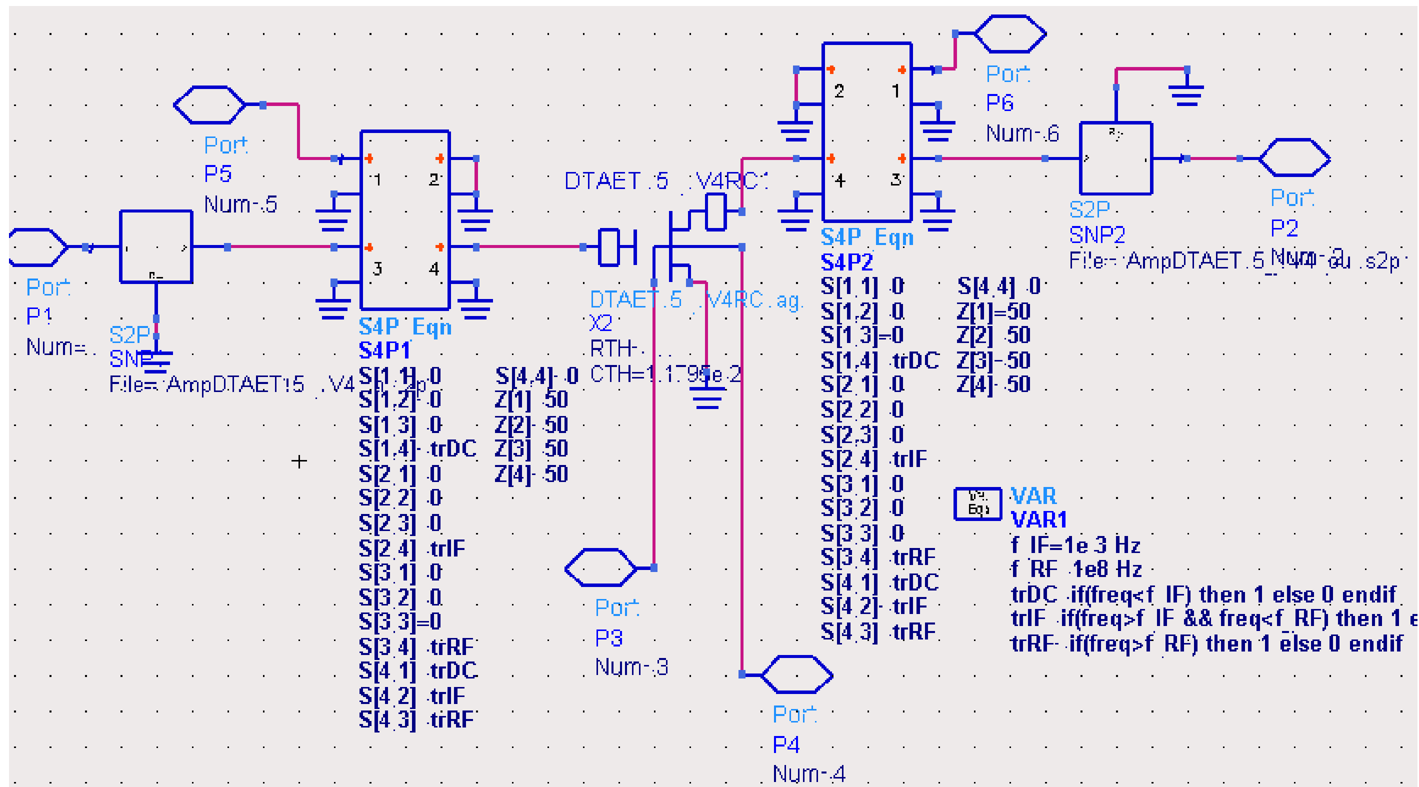

4-port S-parameters are used to control the IF termination which affects the electrical memory effects are reduced

ACPR Degradation for 60W PA

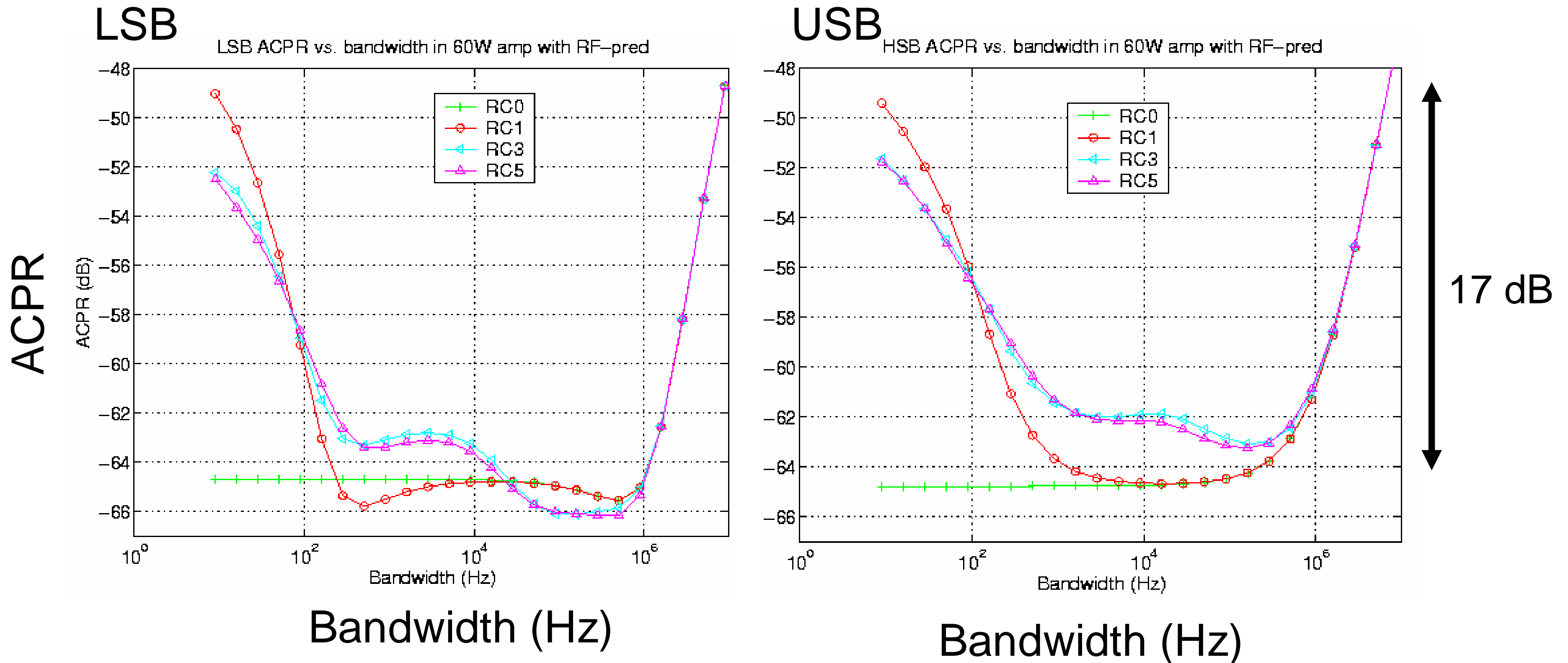

Up to 17 dB degradation of ACPR at low and high bandwidth

Results for Part II: Transient Thermal Modeling and Memory Effects in LDMOSFETs

- Transient thermal response can be obtained form FEM simulation or using an approximate image method extended to predict the 3D transient thermal response of a multi-layer LDMOSFET device.
- The comparison of 1, 3 and 5 stage RC thermal time constant models in circuit simulations shows that the 3 and 5 stage RC models have essentially converged, and provide better accuracy in reporting both fast and slow temperature fluctuations. Larger devices exhibit larger thermal delay.
- Thermal memory effects are found to be dominant over electrical memory effects with bandwith below 100 and 10 kHz in 1W and 60W devices respectively. These thermal fluctuations can be easily handled using adaptive techniques.
- Electrical memory effects were found to dominate over thermal memory effects with bandwidth over 1 MHz
- Dynamic thermal memory effects were demonstrated to have a negligible impact on the linearization of a class A and AB amplifers for wide bandwith sources.
- Fast electrical memory effects are the primary mechanism degrading the linearization performance at wide bandwidth.

Part III: Experimental Results on Memory Effects

Setup used for the PA Characterization

The vectorial source generator used (ESG 4438C) is synchronized with the LSNA 10 MHz reference clock

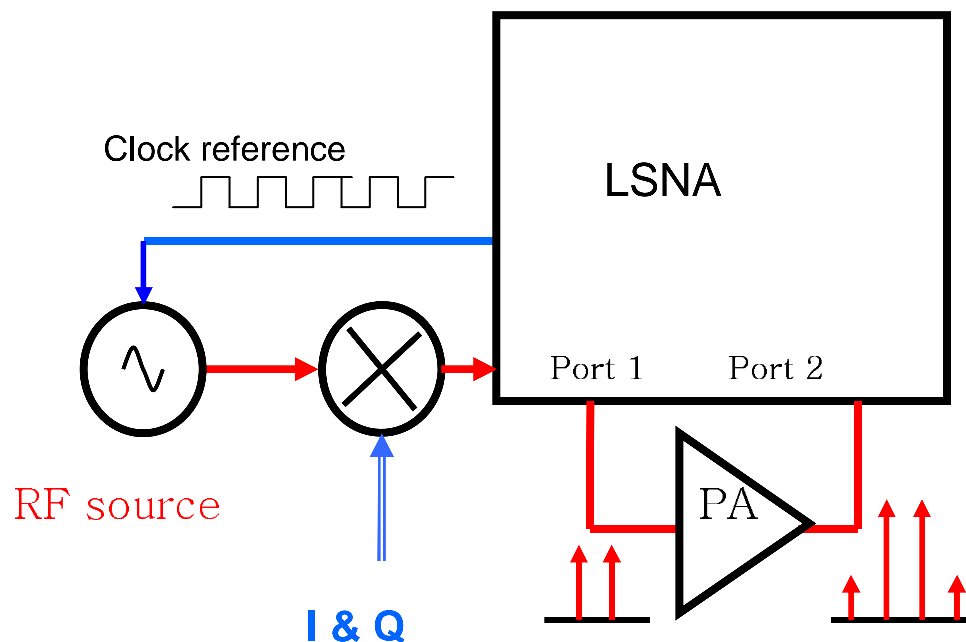

Large signal network analyser

Amplifier Under Test

- Class AB LD-MOSFET PA operating at 895 MHz

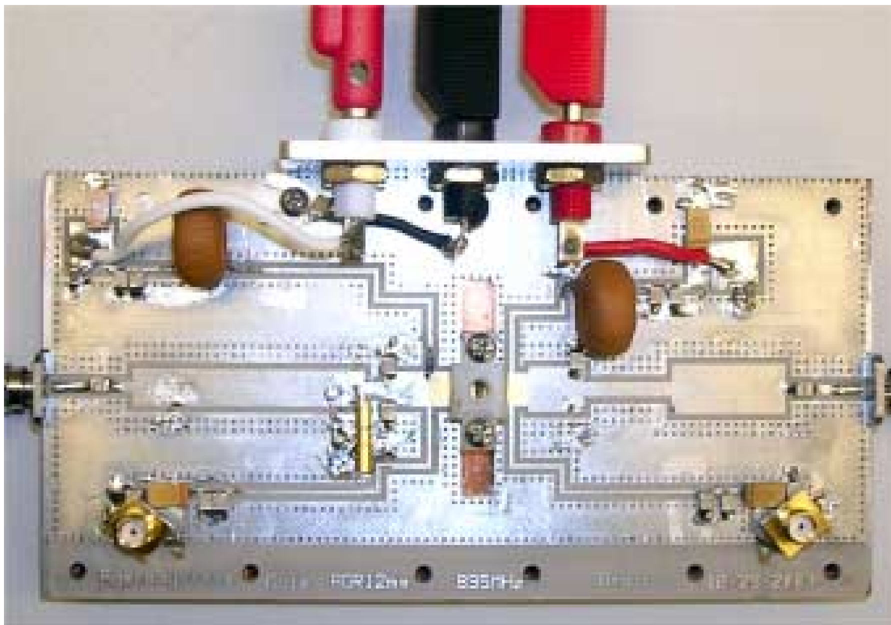

Gain: 13 dB, P1dB: 27.5dBm, PAE =34%,

Extraction of Y_{m3-} & Y_{m3+} using a 2-tone Signal

- The a_1 & b_2 waves are measured with the LSNA

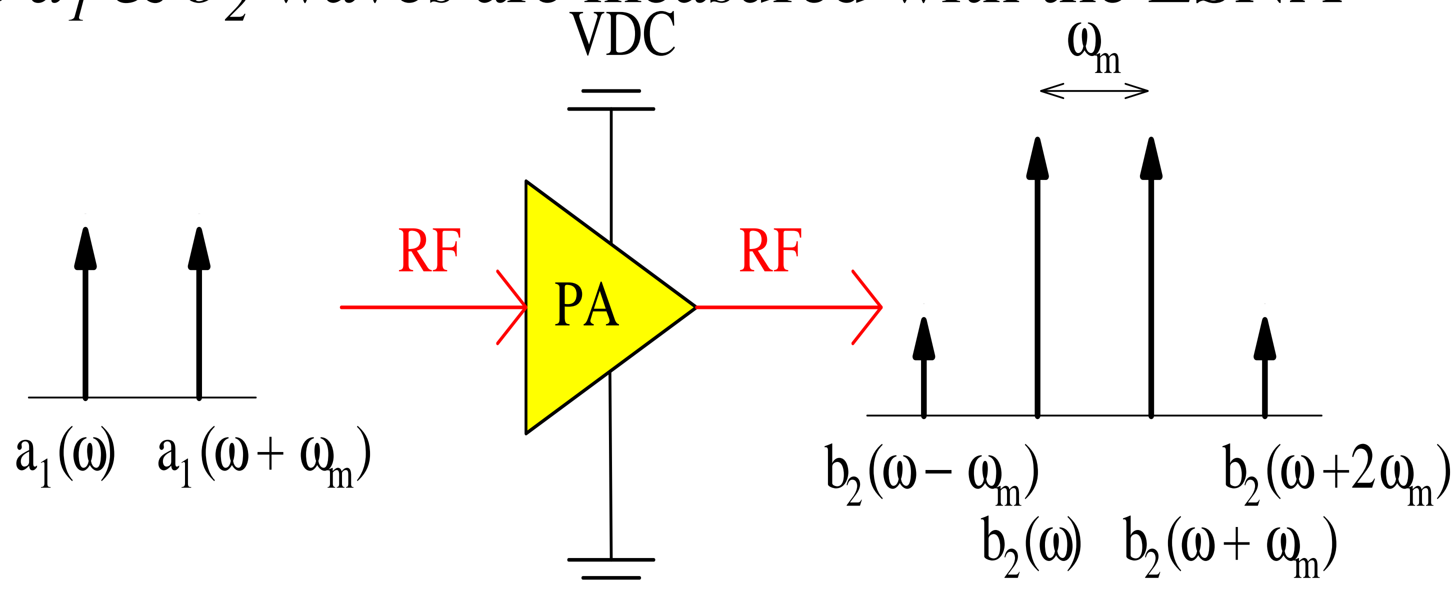

- Generalized Volterra coefficients Y_{m3-} and Y_{m3+} for IMD3:

$$Y_{m3-} = \frac{b_2(\omega - \omega_m)}{a^2{}_1(\omega)a^*{}_1(\omega + \omega_m)} \qquad Y_{m3+} = \frac{b_2(\omega + 2\omega_m)}{a^*{}_1(\omega)a^2{}_1(\omega + \omega_m)}$$

Comparison of Amplitude of Y_{m3-} and Y_{m3+}

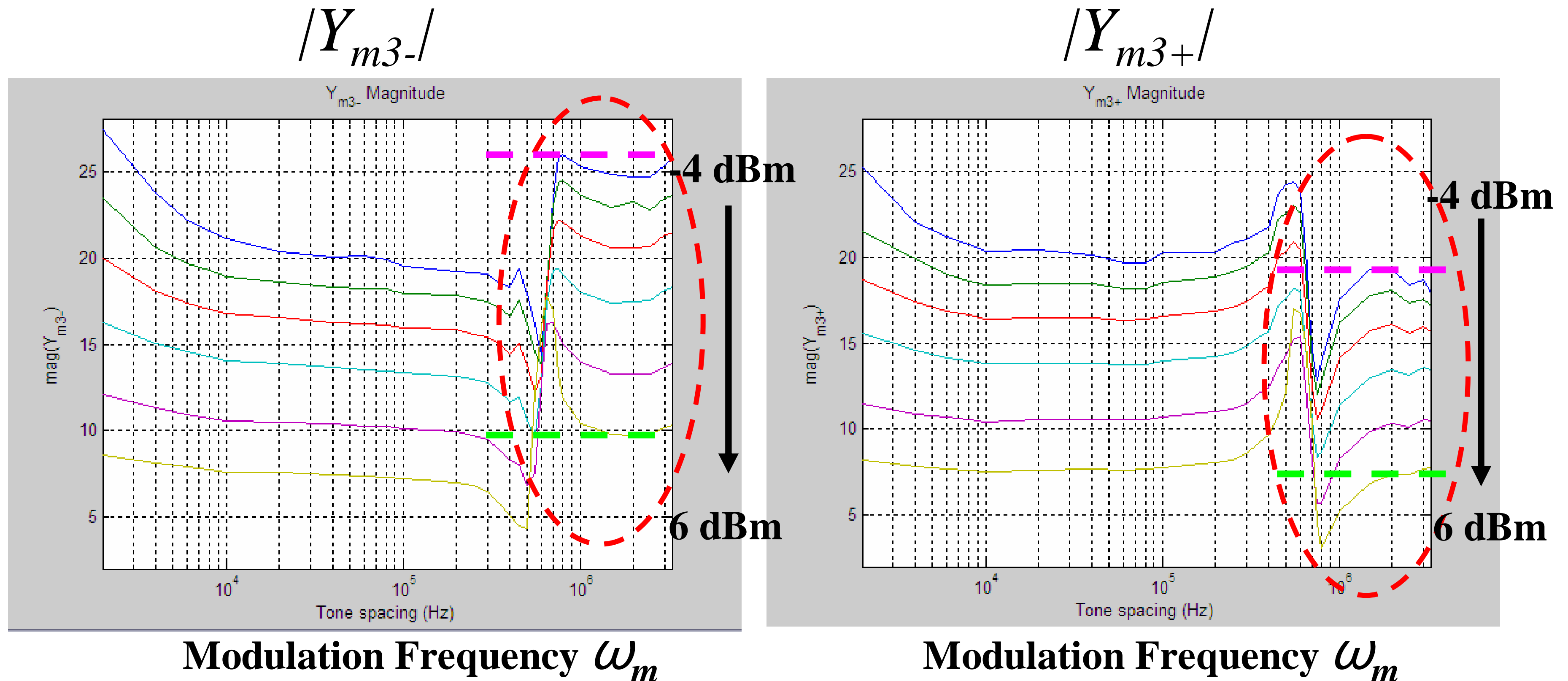

- Comparison of amplitude of Y_{m3-} and Y_{m3+} versus the modulation frequency ω_m for different power levels (-4 ~ 6 dBm).
- The amplitude difference at 3 MHz tone spacing is up to 40%

Comparison of the Phase of Y_{m3-} and Y_{m3+}

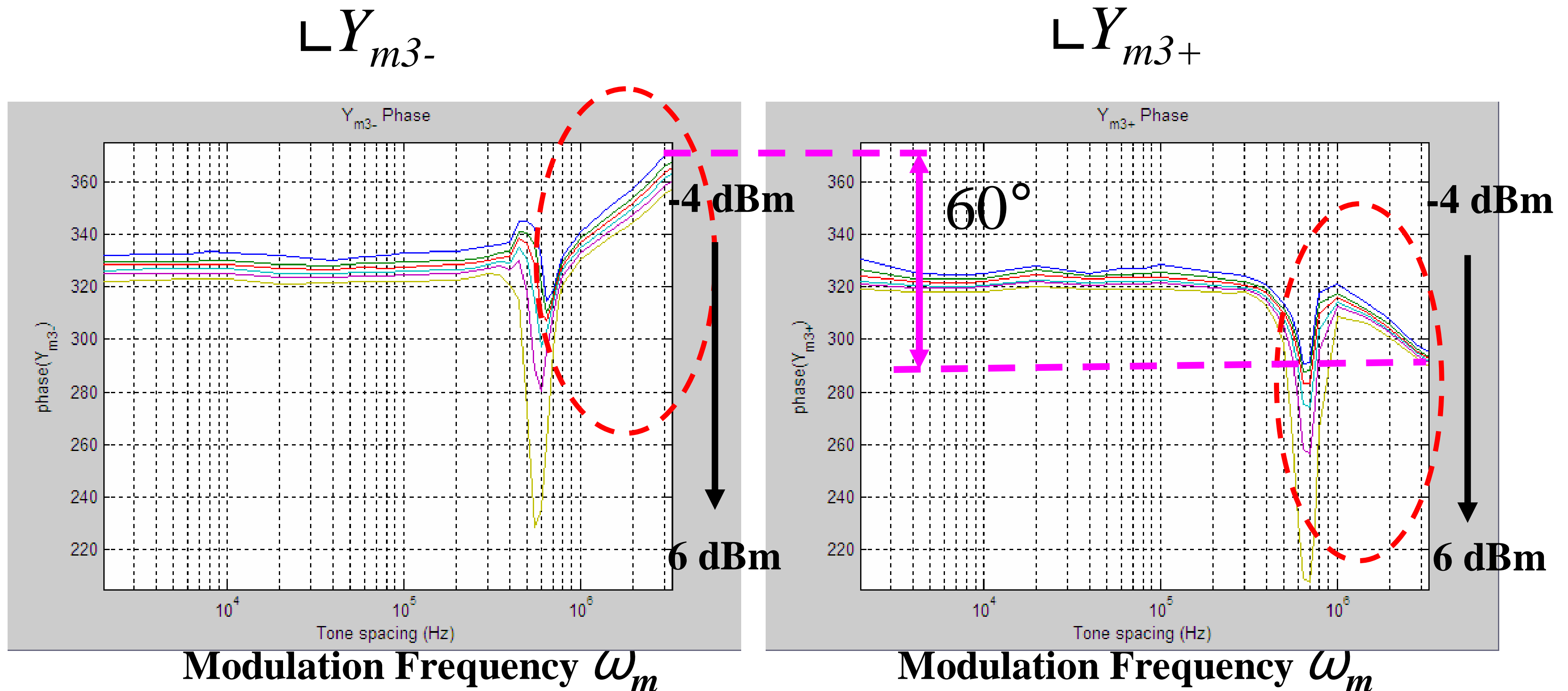

- Comparison of phase of Y_{m3-} and Y_{m3+} versus the modulation frequency ω_m for different power levels (-4 ~ 6 dBm).
- 60° angle difference at 3MHz tone spacing: memory effects

Difference of Y_{m3-} and Y_{m3+}

$|Y_{m3+} - Y_{m3-}|$

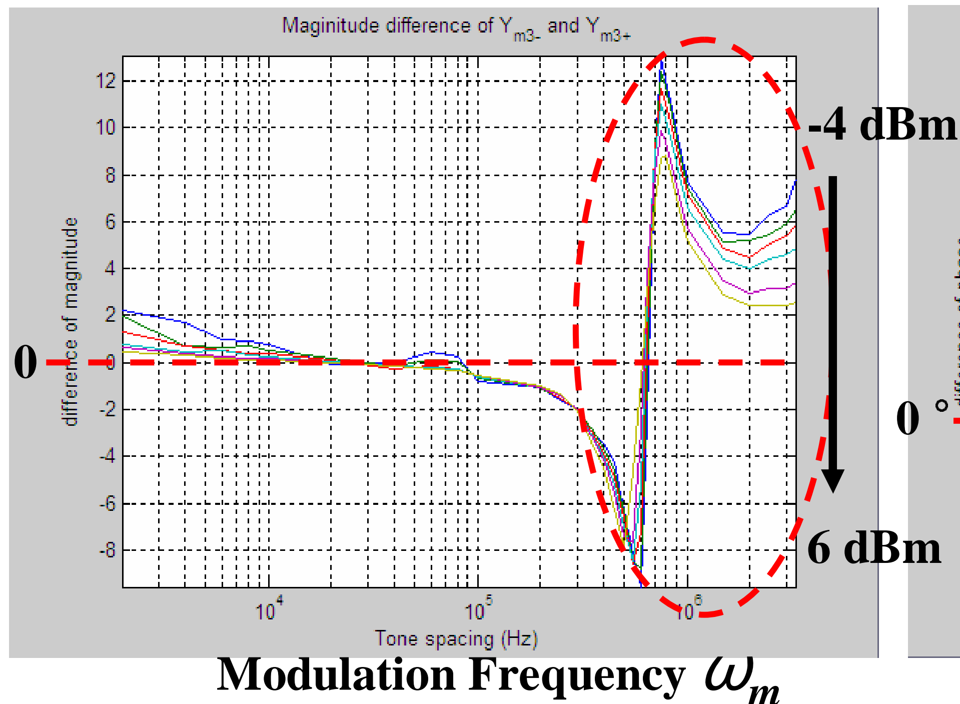

Modulation Frequency ω_m

$\angle(Y_{m3+} - Y_{m3-})$

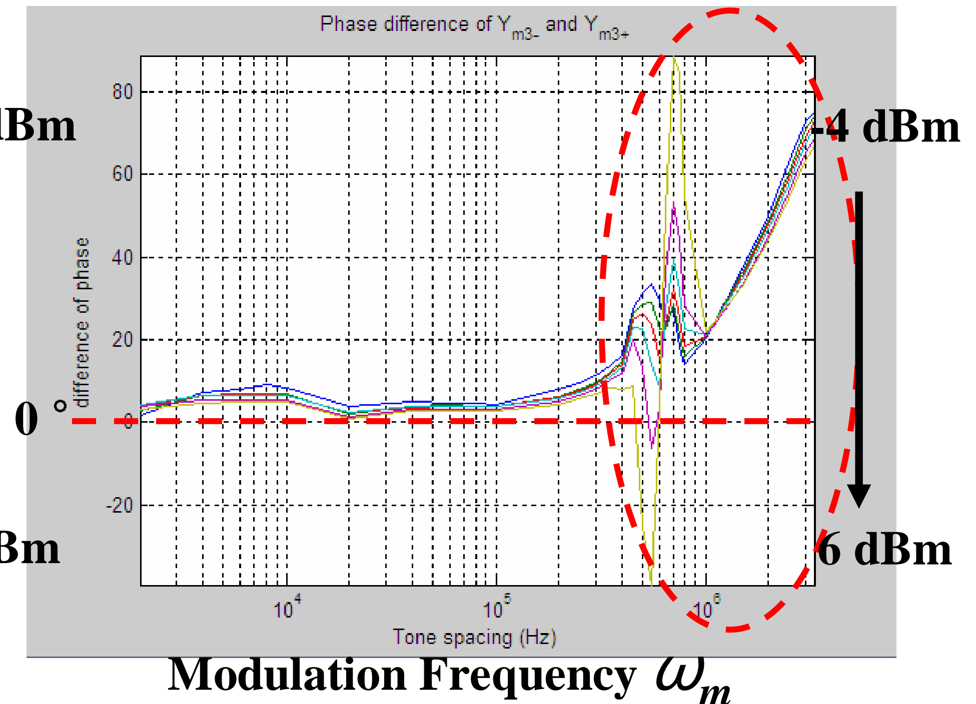

Modulation Frequency ω_m

- The difference in amplitude and phase between Y_{m3-} and Y_{m3+} is mostly significant above 0.3 MHz
- Referred to as a *differential* memory effect

Results from Part III on Non-Linear Measurements

- Below 0.3 MHz the difference in phase and amplitude of Y_{m3-} and Y_{m3+} is small in the PA under test
- Above 0.3 MHz the difference in phase and amplitude increases rapidly with tone spacing
- This indicates the presence of a strong differential memory effect between the LSB & USB for wide bandwidth signals
- There is however no experimental evidence for a strong differential memory effect induced by self-heating.